Supplemental Information

Usp9x controls ankyrin-repeat domain protein homeostasis during dendritic spine development

Sehyoun Yoon, Euan Parnell, Maria Kasherman, Marc P. Forrest, Kristoffer Myczek, Susitha Premarathne, Michelle C. Sanchez Vega, Michael Piper, Thomas H. J. Burne, Lachlan A. Jolly, Stephen A. Wood, and Peter Penzes


A
35 43 135 148 256 289
M. musculus Ank3 GHLEKALDY…HLEVVRFLLDNGAS…HVASKRGNANMVKLLLDRGAKIDAKTRDGLTPLH
H. sapiens Ank3 GHLEKALDY…HLEVVRFLLDNGAS…HVASKRGNANMVKLLLDRGAKIDAKTRDGLTPLH
R. norvegicus Ank3 GHLEKALDY…HLEVVRFLLDNGAS…HVASKRGNANMVKLLLDRGAKIDAKTRDGLTPLH
X. tropicalis Ank3 GNLEKALDY…HLEVVKFLLDNGAS…HVASKRGNANMVKLLLDRGSKIDAKTRDGLTPLH
D. rerio Ank3 GNLEKVLDY…HLDVVRFLLENNSS…HVASKRGNGNMVKLLLDRGSKIEAKTKDGLTPLH
M. musculus Ank2 GNLDKVVEY…HIDVVKYLLENGAN…HVASKRGNTNMVKLLLDRGGQIDAKTRDGLTPLH
H. sapiens Ank2 GNLDKVVEY…HIDVVKYLLENGAN…HVASKRGNTNMVKLLLDRGGQIDAKTRDGLTPLH
R. norvegicus Ank2 GNLDKVVEY…HIDVVKYLLENGAN…HVASKRGNTNMVKLLLDRGGQIDAKTRDGLTPLH
X. tropicalis Ank2 GNLDKVVEY…HIDVVKYLLETGAN…HVASKRGNTNMVKLLLDRGGQIDAKTRDGLTPLH
D. rerio Ank2 GNIDKVLEY…HLDVVRYLLENGGN…YMASQENHLDVVRYLLENGGNQSIATEDGFTPLA
D. melanogaster Ank2 GNLERVLEH…HVDAARILLYHRAP…HVAAKWGKTNMVSLLLEKGGNIEAKTRDGLTPLH

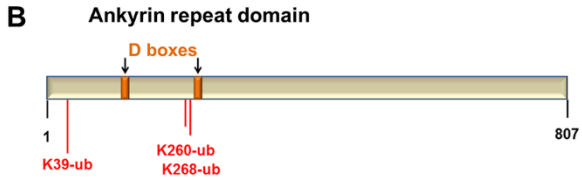
B
Ankyrin repeat domain
D boxes
1
807
K39-ub
K260-ub
K268-ub

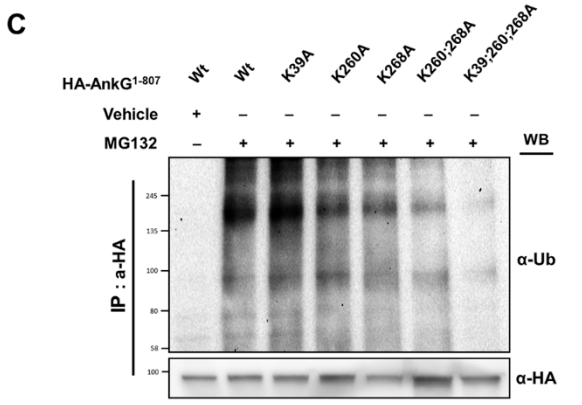
C
HA-AnkG1-807
Wt
Wt
K39A
K260A
K268A
K260;268A
K39;260;268A
Vehicle + – – – – – –
MG132 – + + + + + +
WB
IP : a-HA
245
135
100
80
58
100
α-Ub
α-HA

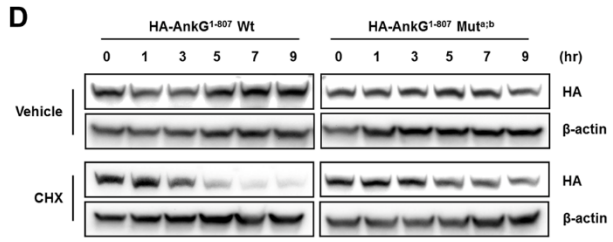
D
HA-AnkG1-807 Wt
HA-AnkG1-807 Mut a;b
0 1 3 5 7 9
0 1 3 5 7 9
(hr)
Vehicle
CHX
HA
β-actin
HA
β-actin

Figure S1: Related to Figure 1. APC-mediated ubiquitinated ankyrin-G

(**A**) Ubiquitinated lysine sites and the second D-box of ankyrin-G are conserved between ankyrin-B and ankyrin-G, and also conserved across different species. (**B**) Diagram of ubiquitinated lysine sites of ankyrin-G (**C**) The ubiquitinated lysine sites of ankyrin-$G^{1\text{-}807}$. HEK293T cells were transfected with HA-ankyrin-$G^{1\text{-}807}$ or point-mutated constructs. At 24 h post-transfection, the transfected cells were treated with 10 μM MG132 for an additional 16 h before harvesting for immunoprecipitation with α-HA. The ubiquitinating ankyrin-G was detected using the anti-Ub antibody. (**D**) HEK293T cells were transfected with HA-ankyrin-$G^{1\text{-}807}$ or the D-box mutant. At 24 h post-transfection, the transfected cells were treated with 20 μg/ml cycloheximide in HA-ankyrin-$G^{1\text{-}807}$ Wt or HA-ankyrin-$G^{1\text{-}807}$ $Mut^{a;b}$ overexpressing cells.

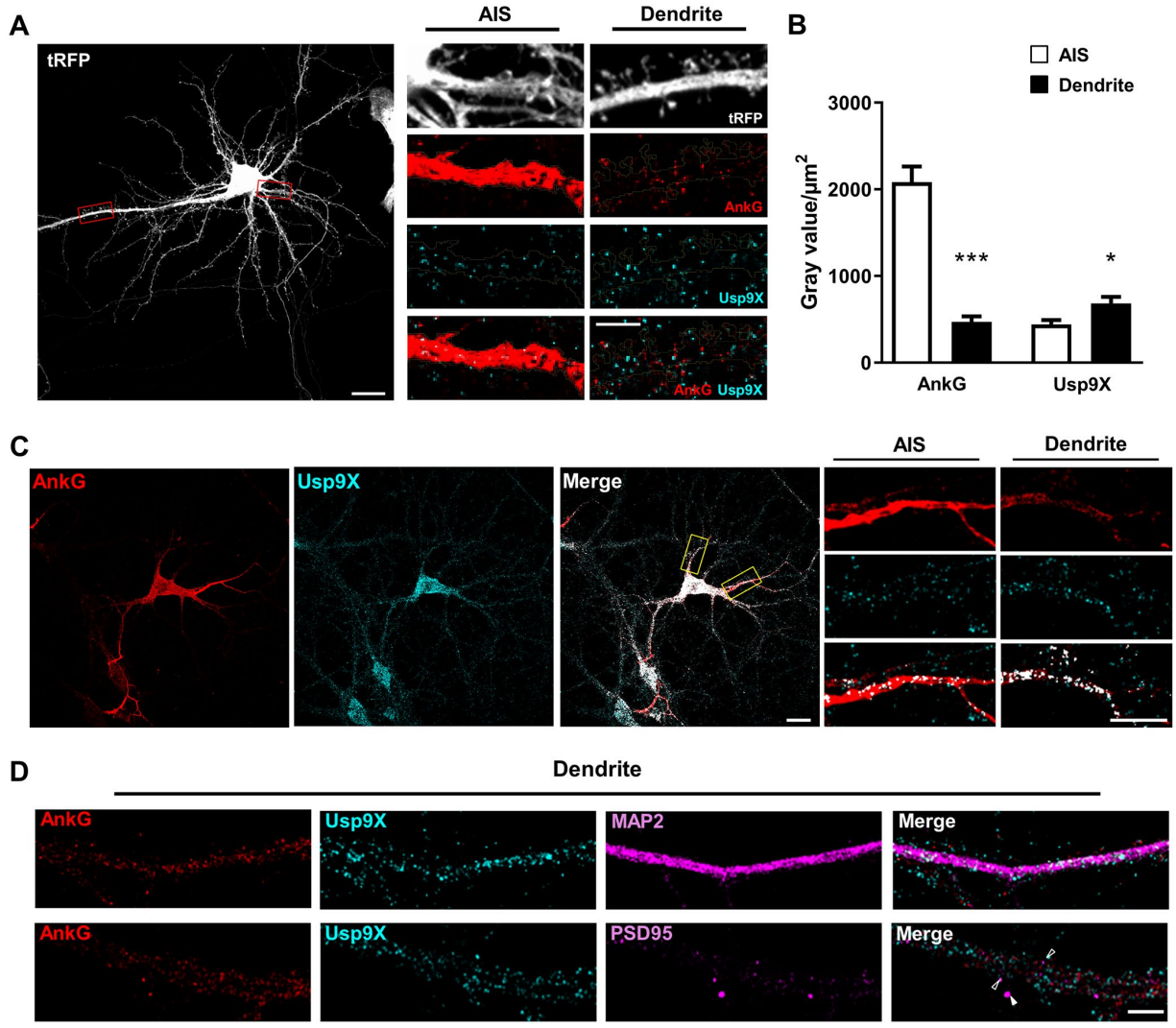

Figure S2: Related to Figure 2. Expression patterns of ankyrin-G and Usp9X in cortical cultured neurons.

(**A**) Confocal images of tRFP transfected neurons immunostained for ankyrin-G and Usp9X. Scale bar, 20μm (for the left panel) and 5μm (for right panel). (**B**) Bar graph comparing intensities of ankyrin-G and Usp9X in the axon initial segment (AIS) and dendrite of primary cultured cortical neurons (n = 9 cells; *p = 0.0169; ***p < 0.001; Two-way ANOVA followed by Bonferroni post-tests. All data represent mean ± SEM. (**C**) Confocal image of a neuron showing the AIS and dendrite. Scale bar, 20μm (left); 10 μm (right). (**D**) Confocal images of neurons immunostained for ankyrin-G, Usp9X, and MAP2 or PSD95. Arrowheads show co-localized puncta. Scale bar, 5μm.

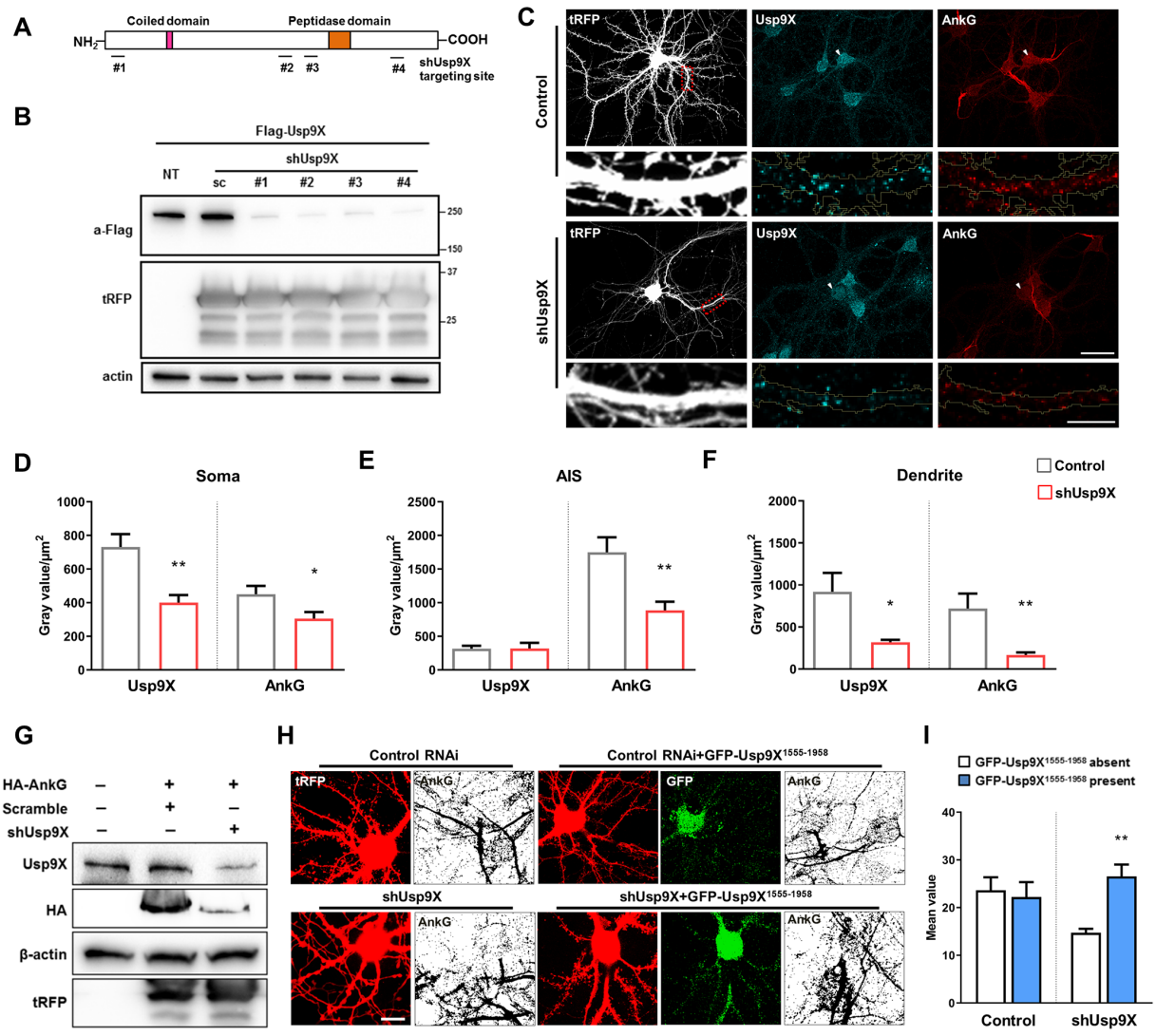
A
Coiled domain
Peptidase domain
NH2
COOH
#1
#2
#3
#4
shUsp9X targeting site
B
Flag-Usp9X
shUsp9X
NT
sc
#1
#2
#3
#4
a-Flag
tRFP
actin
250
150
37
25
C
Control
shUsp9X
tRFP
Usp9X
AnkG
D
Soma
Gray value/μm2
1000
800
600
400
200
0
**
*
Usp9X
AnkG
E
AIS
2500
2000
1500
1000
500
0
**
F
Dendrite
Control
shUsp9X
2000
1500
1000
500
0
*
**
G
HA-AnkG
Scramble
shUsp9X
Usp9X
HA
β-actin
tRFP
H
Control RNAi
Control RNAi+GFP-Usp9X1555-1958
shUsp9X
shUsp9X+GFP-Usp9X1555-1958
tRFP
AnkG
GFP
I
GFP-Usp9X1555-1958 absent
GFP-Usp9X1555-1958 present
Mean value
40
30
20
10
0
**
Control
shUsp9X

Figure S3: related to Figure 3. The effect of shUsp9X on the expression level of ankyrin-G

(**A**) Diagram of target sites of candidate Usp9X RNAi constructs. (**B**) Knock-down of Flag-Usp9X in HEK293T cells. SDS-PAGE and western blot of lysates from HEK293T cells expressing Flag-Usp9X alone or with control or candidate RNAi constructs. RNAi construct 4 was used for knockdown experiments. (**C**) Confocal images of neurons expressing control or Usp9X RNAi (shUsp9X) and immunostained with antibodies to ankyrin-G (red) and Usp9X (cyan). Arrowhead indicates control or shUsp9X expressed neuron. Scale bar, 40 μm (upper panel); 5 μm (lower panel). (**D-F**) Graph comparing intensities of ankyrin-G and Usp9X fluorescence in the soma or AIS or dendrite of cultured cortical neurons expressing control or shUsp9X constructs (n = 9 per each condition; *$p < 0.05$; **$p < 0.01$; followed by two-tailed unpaired Student's t-test). (**G**) Representative western blot for Usp9X-dependent expression level of ankyrin-G. N2a cells were transfected with HA-ankyrin-G and control or Usp9X RNAi constructs. At 48 h post-transfection, the transfected cells were harvested for immunoblotting. (**H**) Confocal images of control and knockdown neurons co-expressing GFP-Usp9X$^{1555\text{-}1958}$ construct. The signal of ankyrin-G was thresholded at an identical value. Scale bar, 10 μm. (**I**) Graph comparing intensities of ankyrin-G fluorescence in the soma of cortical neurons expressing control or shUsp9X constructs (n = 8 per each condition; **$p < 0.01$). Repeated measures two-way ANOVA followed by Bonferroni post-tests. All data represent mean ± SEM.

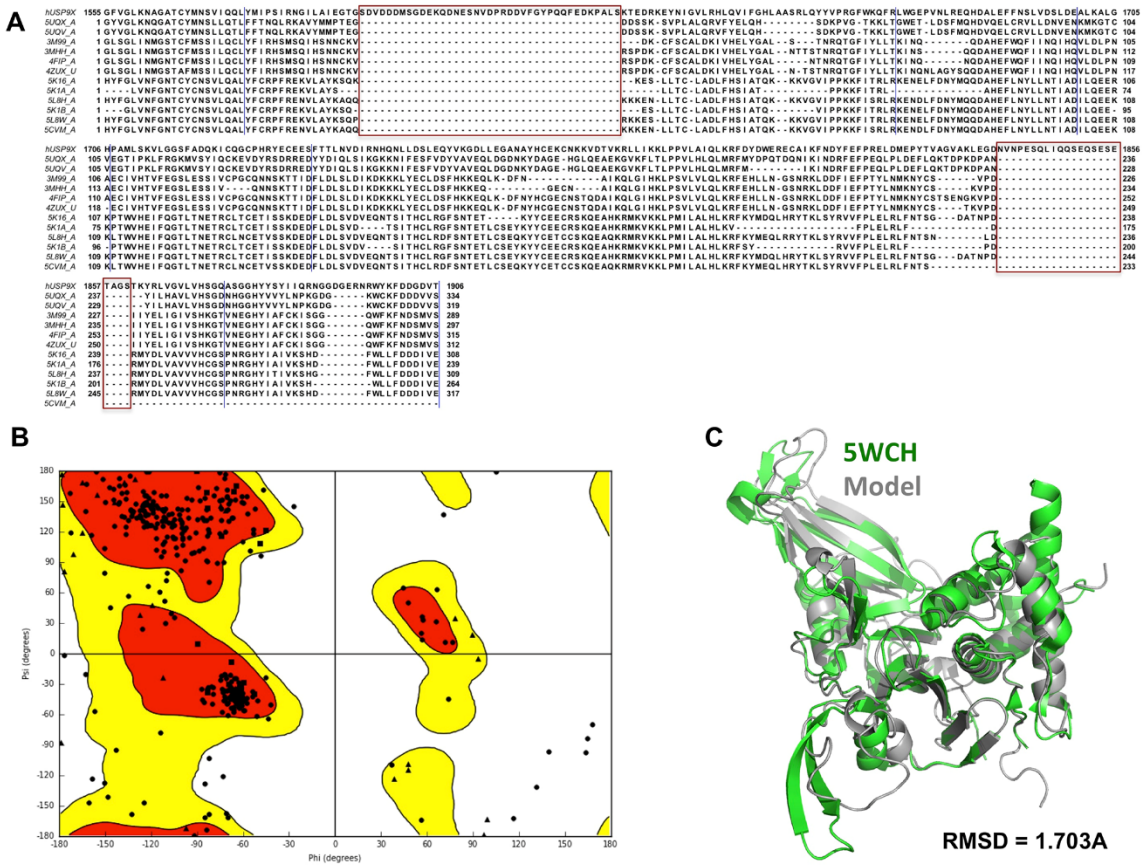

Figure S4: Related to Figure 4. Homology model generation.

(**A**) The sequence of human *USP9X* (*hUSP9X*) DUB domain 1555-1906 was aligned to multiple known DUB structures in order to generate a homology model. Insertions into USP9X (indicated by red squares) with no structural templates were modelled ab initio. Blue lines indicate regions of aligned structural templates not used for modeling, due to absence from *USP9X*. (**B**) Ramachandran plot of novel model showing > 95% amino acids is within accepted backbone torsion angles. (**C**) Alignment of conserved structural elements of homology model generated with Usp9X crystal structure 5WCH showing root mean square deviation between backbone carbons. Regions generated ab initio were not aligned, as these regions are absent from crystal structure 5WCH, likely due to flexibility or crystallization methods.

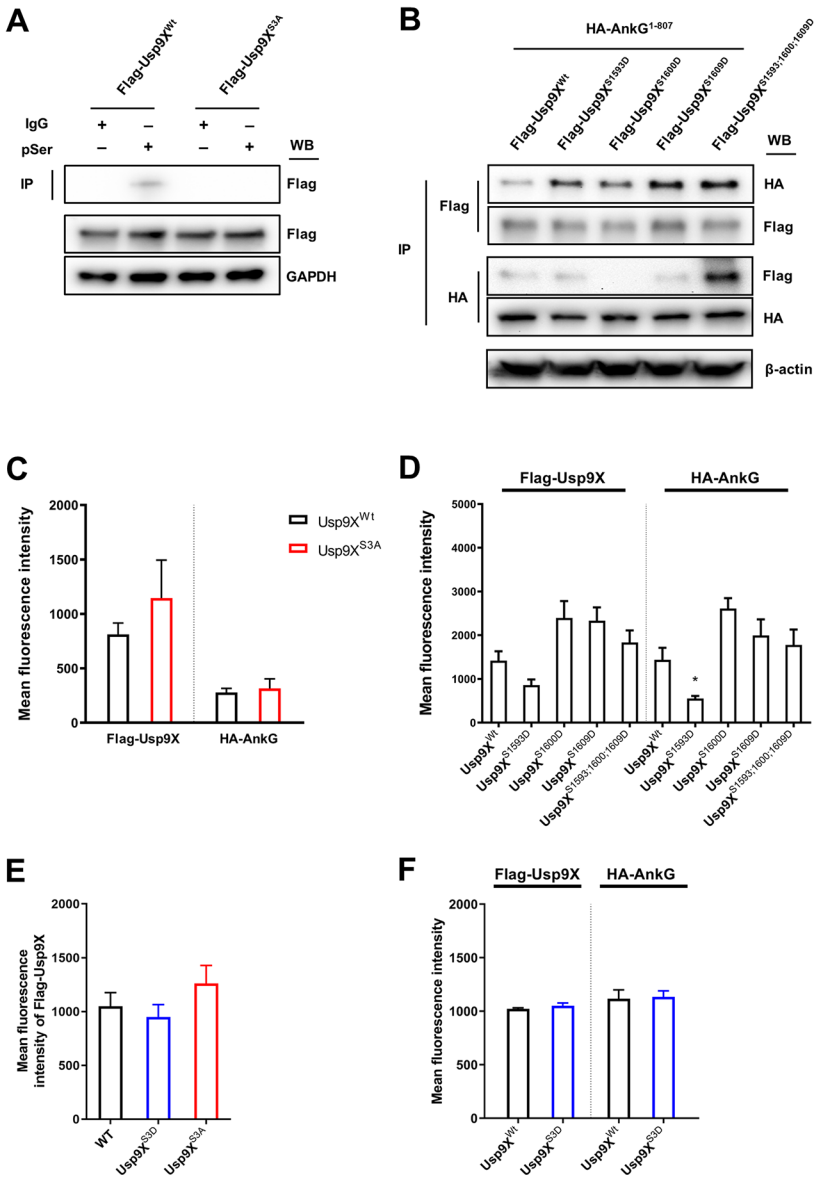
A
Flag-Usp9X^Wt
Flag-Usp9X^S3A
IgG
pSer
WB
IP
Flag
Flag
GAPDH
B
HA-AnkG^1-807
Flag-Usp9X^Wt
Flag-Usp9X^S1593D
Flag-Usp9X^S1600D
Flag-Usp9X^S1609D
Flag-Usp9X^S1593;1600;1609D
WB
IP
Flag
HA
Flag
Flag
HA
HA
β-actin
C
Mean fluorescence intensity
Usp9X^Wt
Usp9X^S3A
Flag-Usp9X
HA-AnkG
D
Flag-Usp9X
HA-AnkG
Mean fluorescence intensity
Usp9X^Wt
Usp9X^S1593D
Usp9X^S1600D
Usp9X^S1609D
Usp9X^S1593;1600;1609D
E
Mean fluorescence intensity of Flag-Usp9X
WT
Usp9X^S3D
Usp9X^S3A
F
Flag-Usp9X
HA-AnkG
Mean fluorescence intensity
Usp9X^Wt
Usp9X^S3D

Figure S5: Related to Figure 4. The effect of phosphomimetic mutants of Usp9X on the interaction with ankyrin-G and the expression levels of transfected constructs.

(**A**) Representative Western blot of co-immunoprecipitation experiments of the Flag-Usp9X$^{1555-1958}$ (Flag-Usp9X^{Wt}) or Flag-Usp9X^{S3A} constructs with α-phosphoserine from HEK293T cells. (**B**) Representative Western blot of the HA-ankyrin-G$^{1-807}$ with co-expressed Flag-Usp9X$^{1555-1958}$ Wt or S1593D, S1600D, S1609D, S3D from HEK293T cells. (**C**) Measurement of mean fluorescence intensity from confocal images. Co-expressed HA-ankyrin-G$^{1-807}$ and Flag-Usp9X$^{1555-1958}$ Wt or S3A signals in HEK293T cells were measured through outlining cellular boundary by a volumetric way (0.4 μm interval and 5.2 μm depth; Usp9X^{Wt} control, n = 16; Usp9X^{S3A} control, n = 9). The graph is related to Figure 4C. (**D**) Measurement of mean fluorescence intensity from confocal images. Co-expressed HA-ankyrin-G$^{1-807}$ and Flag-Usp9X$^{1555-1958}$ Wt, S1593D, S1600D, S1690D, or S3D signals in HEK293T cells were measured through outlining cellular boundary by a volumetric way (0.4 μm interval and 4.8 μm depth; n=20 from each condition; *$p < 0.05$). Two-way ANOVA followed by Bonferroni post-tests. The graph is related to Figure 4D. (**E**) Graph comparing mean intensities of Flag-Usp9X$^{1555-1958}$ Wt, S3D, or S3A fluorescence in dendrites of cortical neurons (n = 16 from each condition). The graph is related to Figure 4H. (**F**) Graph comparing mean intensities of HA-ankyrin-G and Flag-Usp9X$^{1555-1958}$ Wt or S3D fluorescence in dendrites of cortical neurons (n = 13 from each condition). The graph is related to Figure 4J. All data represent mean ± SEM.

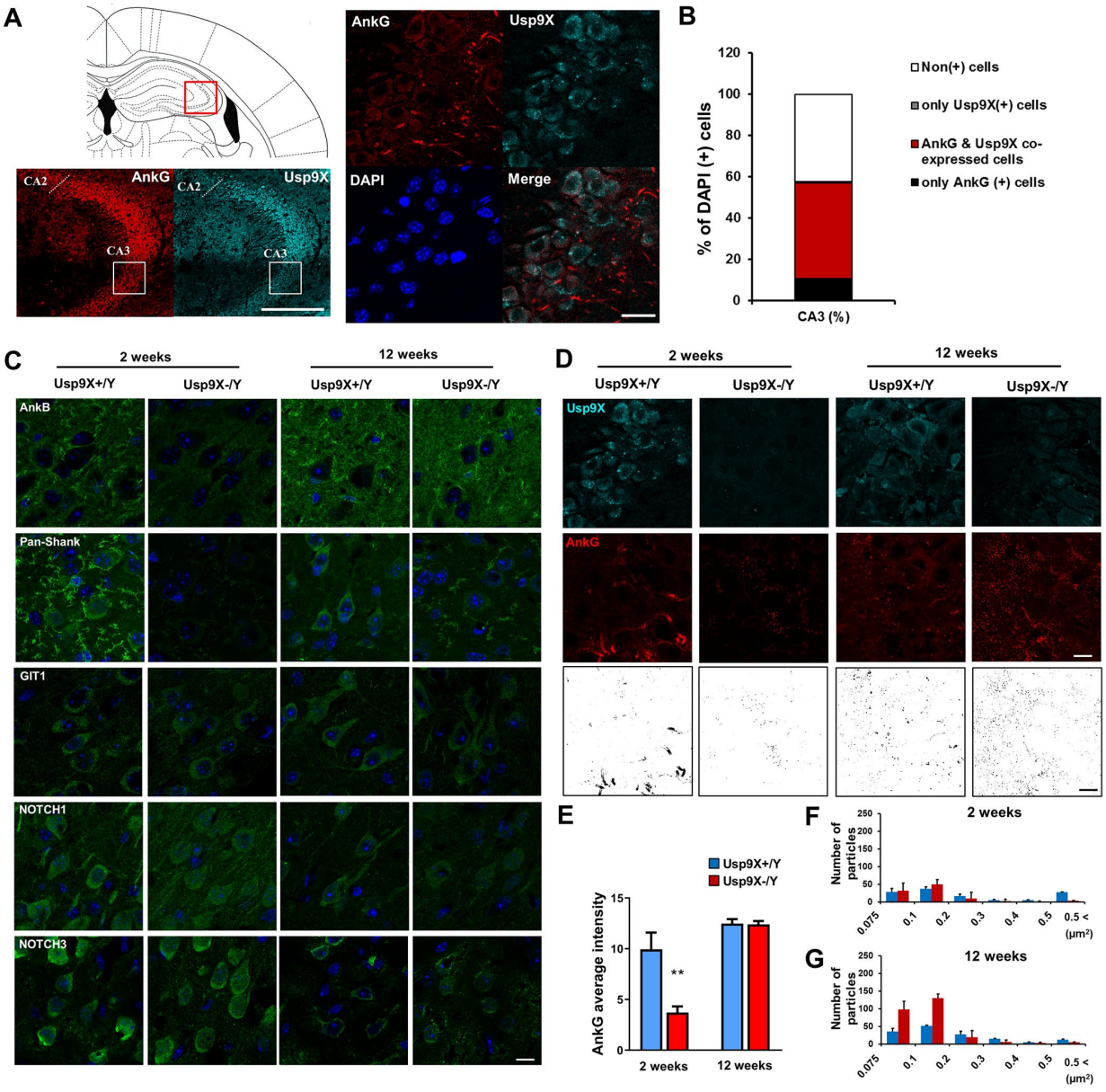
A
AnkG
Usp9X
CA2
CA3
DAPI
Merge
B
% of DAPI (+) cells
CA3 (%)
Non(+) cells
only Usp9X(+) cells
AnkG & Usp9X co-expressed cells
only AnkG (+) cells
C
2 weeks
12 weeks
Usp9X+/Y
Usp9X-/Y
AnkB
Pan-Shank
GIT1
NOTCH1
NOTCH3
D
Usp9X
AnkG
E
AnkG average intensity
**
F
2 weeks
Number of particles
(μm²)
G
12 weeks

Figure S6: Related to Figure 5 and 6. Expression patterns of ankyrin-G and Usp9X

(**A**) Double-immunohistochemical staining of ankyrin-G (detected in green) with Usp9X (detected in red) in the hippocampus (Bregma -1.70 mm) of 12 weeks old mouse brain. Hippocampal expression patterns of ankyrin-G and Usp9X are shown in the left panel (Scale bar, 200 μm) and magnified CA3 region is shown in right panel as a representative image (Scale bar, 20 μm). (**B**) Representative graph of the fraction of ankyrin-G (red and black) or Usp9X (grey and red)-positive cells and quantification of the two cell types (n = 5) in CA3 of the hippocampus. The red bar represents co-expressed cells of both ankyrin-G and Usp9X. The graph is shown with mean values. (**C**) Representative image of immunohistochemical staining with ankyrin-B, Pan-Shank, GIT1, Notch1, or Notch3 (detected in green) in the layer III of cortex from 2 or 12 weeks old mouse brain of $Usp9X^{+/Y}$ or $Usp9X^{-/Y}$ mice (Scale bar, 10 μm). (**D**) Representative image of double-immunohistochemical staining with ankyrin-G (detected in green) and Usp9X (detected in red) in the hippocampus of 2 or 12 weeks old mouse brain from $Usp9X^{+/Y}$ or $Usp9X^{-/Y}$ mice (Scale bar, 200 μm, top). CA3 specific expression patterns of ankyrin-G and Usp9X are magnified (Scale bar, 20 μm, bottom). (**E**) The ankyrin-G average intensity is measured in each group by ImageJ (n = 4 from 4 mice per each group; $^{**}p<0.01$). Two-way ANOVA followed by Bonferroni post-tests. (**F-G**) The number of ankyrin-G particles based on the bottom images of (D) is counted and categorized by particle size; less than 0.075 μm^2 is excluded for analysis (n = 4 from 4 mice per each group).

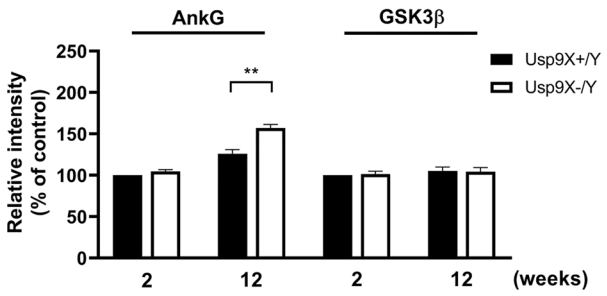

Figure S7: Related to Figure 6. Basal intensity of Western blot of immunoprecipitated ankyrin-G or GSK3β by α-Ub from Figure 6B. Intensity of Western blot of immunoprecipitated ankyrin-G or GSK3β by α-Ub (Fig. 6B) was measured ($Usp9X^{+/Y}$, n = 4 and $Usp9X^{-/Y}$, n = 3 in 2 weeks old; $Usp9X^{+/Y}$, n = 4 and $Usp9X^{-/Y}$, n = 4 in 12 weeks old). **$p < 0.01$; Two-tailed unpaired t-test was performed.

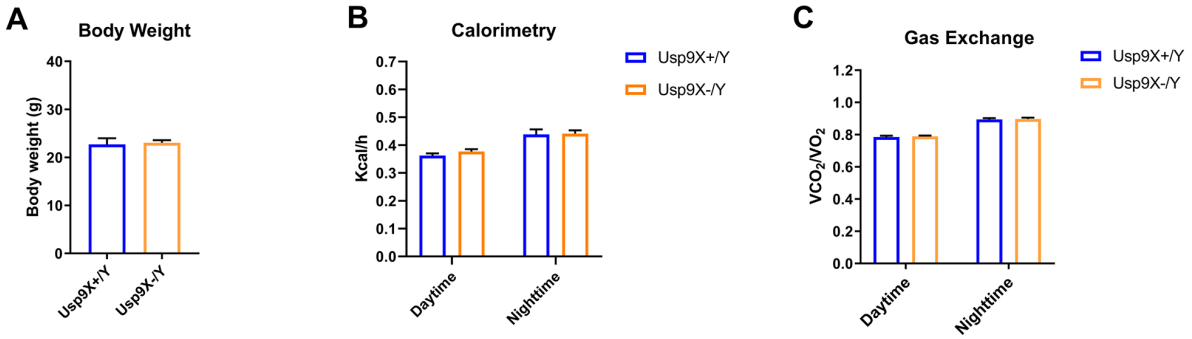

D

Family	Variant Details			Denovo	Gnomad Allele Frequency	Prediction Algorithms					
	Chromosome	cDNA	Protein			SIFT		Polyphen2_HVAR		CADD	GERPN
	ChrX GRCh37(hg19)	NM_001039590.2	NP_001034679.2			Score	Pred	Score	Pred	Score	Score
USA 13	41029757A>G	c.4718A>T	p.Gln1573Leu	Yes	0	0.76	T	0.952	Pr	22.8	5.49
France 1	41075489G>A	c.5669G>A	p.Gly1890Glu	No	1.12E-05	0.267	T	0.002	B	15.6	4.93
USA 4	41075489G>A	c.5669G>A	p.Gly1890Glu	No	1.12E-05	0.267	T	0.002	B	15.6	4.93

E

F

	USA 13	France 1	USA 4
Variant	p.Gln1573Leu	p.Gly1890Glu	p.Gly1890Glu
Neurological Features			
ID	n/a	Yes	Yes
DD	Yes	Yes	
Speech Delay	Yes	Yes	
Autistic Behaviour	No	Yes	Yes
Seizures / Epilepsy	No	No	
Hypotonia	Yes	n/a	
Motor Disability	Yes	Yes	
Ataxia	No	N/A	
Visual impairment	Yes	Yes	
Deafness	No	n/a	

G

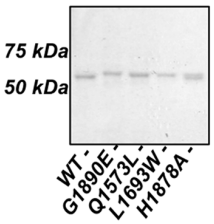

H

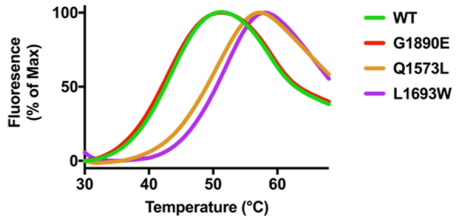

Figure S8: Related to Figure 7. USP9X missense variants within the catalytic domain are associated with neurodevelopmental disorders.

(**A**) Body weight is unchanged across genotypes. (**B**) The amount of kilocalories consumed per an hour. (**C**) The amount of gas exchange. $Usp9X^{+/Y}$, n=6; $Usp9X^{-/Y}$, n=12 from all experiments. (**D**) Two unique missense variants were identified through whole exome or whole genome sequencing with no other plausible variants discovered. One of the variants arose de novo, the other was maternally inherited. All variants are extremely rare, not seen in Gnomad resource (138K exomes/genomes of individuals without neurodevelopmental disorders). All variants were predicted to be potentially disease causing by CADD (CADD score ≥ 20), and affect highly conserved residues (GERPN > 5). Effect on protein structure was predicted to be variable (SIFT: T=tolerated; Polyphen: B=benign, Pr=probably damaging.). (**E**) Missense variants affect highly conserved amino acids. Multiple species alignment of USP9X protein sequence showing location of variants. Numbers relate to human USP9X reference sequence. (**F**) *USP9X* variants are associated with various neurodevelopmental disorders. Summary of neurological features associated with each case. ID: intellectual disability; DD: developmental delay; ASD: autism spectrum disorder. (**G**) Mouse Usp9X and the indicated mutants were recombinantly expressed, purified to greater than 95% purity and equilibrated as assessed by SDS page. Equilibrated protein was used for all subsequent experiments. (**H**) Fluorescence thermal shift was performed using 0.5 μg of the indicated mutants were incubated with Sypro orange (5x concentration) and subjected to a melt curve from 4–95 °C with fluorescence recorded at 0.5 °C intervals (samples run in quadruplicate with data normalized to max fluorescence and cropped to melt peak).

Table S1: Related to Figure 1. The prediction of D-box and KEN box results for the mouse ankyrin-G (National Center for Biotechnology Information accession number NM_146005) are shown.

Position	Peptide	Score	Cutoff	Type
140 - 143	ENHLEVV**RFLL**DNGASQS	2.486	0	D-box
282 - 285	AKIDAKT**RDGL**TPLHCGA	3.608	0	D-box
1028 - 1031	ITCRLVK**RHKL**ANPPPMV	3.486	0	D-box
1177 - 1180	GALTKRI**RVGL**QAQPVPE	3.081	0	D-box
1283 - 1286	FTTNVSA**RFWL**ADCHQVL	3.095	0	D-box
1392 - 1394	VFNFYSF**KEN**RLPFSIK	10.75	0	KEN-box
1773 - 1776	AMLNRVQ**RAEL**AMSSLAG	4.027	0	D-box
1865 - 1867	DIGKQSI**KEN**LKPKTHG	10.727	0	KEN-box
1925 - 1928	TTADGKA**RLNL**QEEEGST	3.568	0	D-box

Residues defining the D-box and KEN box are marked in bold.

Table S3: Related to Figure 5. The ubiquitinated lysine sites of ANKRD in ANKRD containing psychiatric risk genes

Gene symbol	ACC_ID	The N. of amino acids	ANKRD	Human	Mouse (homologous sequence)	Rat (homologous sequence)	Ub-Lysine	PSD protein	D-box	KEN box
ANK3	Q12955	4377	73~825		260, 268		yes	yes	yes	no
TRANK1	O15050	2925	168~575	561			yes	no	yes	no
ABTB1	Q969K4	478	1~64			N/A	no	no	yes	no
AGAP1	Q9UPQ3	857	768~830				no	yes	yes	no
AGAP2	Q99490	1192	1090~1152				no	yes	yes	no
ANK1	P16157	1881	44~795	436, 454, 534	55, 165, 266, 299, 450, 607, 662, 685	63	yes	yes	yes	no
ANK2	Q01484	3957	30~822		46, 52, 118, 223, 275, 330, 382, 572, 749, 802	52, 118	yes	yes	yes	no
ANKDD1A	Q495B1	522	14~385			N/A	no	no	yes	no
ANKFN1	Q8N957	763	136~202				no	no	yes	no
ANKK1	Q8NFD2	765	361~753	702		N/A	yes	no	yes	no
ANKRD11	Q6UB99	2663	167~292				no	no	no	no
ANKRD13B	Q86YJ7	626	47~109				no	no	yes	no
ANKRD17	O75179	2603	233~1414				no	no	yes	no
ANKRD22	Q5VYY1	191	39~163	N/A	N/A	N/A	no	no	yes	no
ANKRD23	Q86SG2	305	143~271			258	yes	no	yes	no
ANKRD27	Q96NW4	1050	396~871	411	764		yes	no	yes	no
ANKRD30B	Q9BXX2	1392	72~233		N/A	N/A	no	no	yes	no
ANKRD50	Q9ULJ7	1429	477~1107				no	no	yes	no
ANKS1A	Q92625	1134	79~275		198		yes	no	no	no
ASAP1	Q9ULH1	1129	600~665				no	yes	no	no
ASAP2	O43150	1006	584~649				no	no	yes	no
ASB1	Q9Y576	335	36~265	69		N/A	yes	no	yes	no

ASB11	Q8WXH4	323	64~256			N/A	no	no	yes	no
ASB14	A6NK59	587	82~449			N/A	no	no	yes	no
ASB15	Q8WXK1	588	110~444		133	N/A	yes	no	yes	no
ASB17	Q8WXJ9	295	146~176			N/A	no	no	no	no
ASB4	Q9Y574	426	74~280				no	no	yes	no
ASZ1	Q8WWH4	475	45~243				no	no	yes	no
BCORL1	Q5H9F3	1711	1455~1549		1491	N/A	yes	no	no	no
BTBD11	A6QL63	1104	603~854			N/A	no	no	yes	no
CTTNBP2	Q8WZ74	1663	709~942				no	yes	yes	no
DAPK1	P53355	1430	378~638				no	yes	yes	no
ESPN	B1AK53	854	1~300				no	no	yes	no
GIT1	Q9Y2X7	761	132~228				no	yes	no	no
GIT2	Q14161	759	132~228				no	no	no	no
HACE1	Q8IYU2	909	64~257				no	no	yes	no
HECTD1	Q9ULT8	2610	395~612	461, 466, 522			yes	no	no	no
KANK1	Q14678	1352	1161~1329				no	no	no	no
LRRK1	Q38SD2	2015	86~222			N/A	no	no	yes	no
MIB1	Q86YT6	1006	430~729	437, 481, 485, 495, 618, 691, 726	485, 726	N/A	yes	no	yes	no
MPHOSPH 8	Q99549	860	600~728	623, 708			yes	no	no	no
NFKBIL1	Q9UBC1	381	64~130			N/A	no	no	no	no
NOTCH1	P46531	2555	1928~2122				no	no	yes	no
NOTCH3	Q9UM47	2321	1838~2000			N/A	no	no	yes	no
POTEH	Q6S545	545	180~404		N/A	N/A	no	no	yes	no
PPP1R13B	Q96KQ4	1090	920~985				no	no	no	no
SHANK1	Q9Y566	2161	212~395			253	yes	yes	yes	no
SHANK2	Q9UPX8	1470	167~392				no	yes	no	no
SHANK3	Q9BYB0	1731	148~345			167	yes	yes	yes	no
TANC1	Q9C0D5	1861	896~1272				no	no	yes	no

TANC2	Q9HCD6	1990	846~1227				no	no	yes	no
TNKS	O95271	1327	181~964	210, 327, 507, 659, 767, 771, 791, 812, 821, 932	320, 500, 576, 784, 805, 806	N/A	yes	no	yes	no
TNKS2	Q9H2K2	1166	57~776	169, 225, 398, 425, 510, 633, 654, 663	58, 425, 633, 654, 655	N/A	yes	no	yes	no
TONSL	Q96HA7	1378	528~626			N/A	no	no	yes	no
TRPC4	Q9UBN4	977	31~170				no	no	yes	no
TRPV4	Q9HBA0	871	237~398		344,352		yes	no	no	no
TRPV5	Q9NQA5	729	44~268		57		yes	no	yes	yes
UACA	Q9BZF9	1416	38~228				no	no	yes	no
YTHDC2	Q9H6S0	1430	506~571				no	yes	no	no

Table S4: Related to Figure 1, 3, 4, and 7, Figure S1, S3, S5, and S8. Sequences of oligos used this study.

Primer name	Reporter name	Sequence
AnkG 1-807 F	HA-AnkG$^{1-807}$	AAGGAATTCGGTACCATGAGTGAAGAGCCAAA
AnkG 1-807 R		GCGGCCGCACTCGAGCTAGGTCATAATTTCCT
AnkG 808-1475 F	HA-AnkG$^{808-1475}$	AAGGAATTCGGTACCATGACCACTACCATCAC
AnkG 808-1475 R		GCGGCCGCACTCGAGCTAACAAGGACTCTGCG
AnkG 1476-1961 F	HA-AnkG$^{1476-1961}$	AAGGAATTCGGTACCATGGAGCGGACGGATAT
AnkG 1476-1961 R		GCGGCCGCACTCGAGCTAGTGGGTTTTCTTCT
AnkG 808-1961 F	HA-AnkG$^{808-1961}$	AAGGAATTCGGTACCATGACCACTACCATCAC
AnkG 808-1961 R		GCGGCCGCACTCGAGCTAGTGGGTTTTCTTCT
Usp9X 1555-1958 F	Flag-Usp9X$^{1555-1958}$	AAGGAATTCGGTACCATGGGATTTGTGGGGCT
Usp9X 1555-1958 R		GCGGCCGCACTCGAGCTATGTGTCCATTCGTT
GFP-AnkG F	GFP-AnkG	TACCGGACTCAGATCATGAGTGAAGAGCCAAA
GFP-AnkG R		GGCGACCGGCCGGTGGTGGGTTTTCTTCTCCA
GFP-Usp9X 1555-1958 F	GFP-Usp9X$^{1555-1958}$	TACCGGACTCAGATCATGGGATTTGTGGGGCTG
GFP-Usp9X 1555-1958 R		GGTGGCGACCGGCCGGTGTGTGTCCATTCGTTC
Usp9X 1547-1962 F	His-Usp9X$^{1547-1962}$	TACTTCCAATCCAATCCCGTTGGACCCCGTCCACC
Usp9X 1547-1962 R		TTATCCACTTCCAATTTAATGACCTATTGTGTCCA TTCGTTCATA
Mut[a]	HA-AnkG$^{1-807}$ Mut[a] GFP-AnkG$^{1-807}$ Mut[a]	CAGGAGAACCACCTGGAAGTCGTCGCGTTTCTTG CGGACAATGGCGCCAGCCAAAGCCTG
Mut[b]	HA-AnkG$^{1-807}$ Mut[b] GFP-AnkG$^{1-807}$ Mut[b]	GGTGCGAAGATCGATGCCAAGACCGCGGACGGTG CGACTCCGTTGCACTGTGGGGCGAGA
K39A	HA-AnkG$^{1-807}$ K39A	CAGGGCACCTGGGCAAGGCCCTTGACT
K260A	HA-AnkG$^{1-807}$ K260A	CACGTTGCCTCGGCGCGAGGAAATGCA
K268A	HA-AnkG$^{1-807}$ K268A	GCAAATATGGTGGCGCTATTGCTGGAC
S1593A	Flag-Usp9X^{S3A}	GAAGGCACAGGTGCTGATGTAGATGATG
S1600A		TAGTGATGTAGATGATGATATGGCTGGGGATGAG AAGC
S1609A		CAGGACAACGAGGCCAATGTTGATCCC
S1593D	Flag-Usp9X^{S1593D} His-Usp9X^{S1593D}	GCCATAGAAGGCACAGGTGATGATGTAGATGATG ATATGTCTGGGG
S1600D	Flag-Usp9X^{S1600D} His-Usp9X^{S1600D}	GATGTAGATGATGATATGGATGGGGATGAGAAGC AGGACAACG
S1609D	Flag-Usp9X^{S1609D} His-Usp9X^{S1609D}	GGATGAGAAGCAGGACAACGAGGACAATGTTGA TCCCAGG
H1878A	His-Usp9X H1878A	GGTCAAGCAAGTGGCGGAGCTTACTATTCTTACA TCATTCAGAGG
Q1573L	Flag-Usp9X^{Q1573L} His-Usp9X^{Q1573L}	ACATGAACTCTGTGATCCTGCAACTCTATATGATC CC
L1693W	Flag-Usp9X^{L1693W} His-Usp9X^{L1693W}	GTTCTTTAATTCTTGGGTGGATAGTTTAGATG
G1890E	Flag-Usp9X^{G1890E} His-Usp9X^{G1890E}	TCATTCAGAGGAATGGAGAGGATGGTGAAAAAA ATCGTTG
His-Usp9X 1547-1962 F	His-Usp9X^{S3A}	TACTTCCAATCCAATCCCGTTGGACCCCGTCCACC AAAAGGATTTGTGGGGCTGAAAAATGCTGG
His-Usp9X 1547-1962 R		GCATATATACTTTTTTATGAACGAATGGACACAAT AGGTCATTAAATTGGAAGTGGATAA

Underline indicates codon altered.